1.1 STABILITY OF NANOPRECIPITATES IN FE-BASE MODEL ALLOYS — L. Tan, Y. Katoh, and L. L. Snead (Oak Ridge National Laboratory)

OBJECTIVE

The objective of this work is to determine the stability of MX-type nanoprecipitates in reduced-activation ferritic (RAF) steels using Fe-base model alloys under thermal, stress, and radiation conditions. This will help understand the failure mechanisms of RAF steels and identify promising strengthening particles for advanced RAF steel development.

SUMMARY

The radiation resistance of TaC, TaN, and VN MX-type nanoprecipitates is being evaluated using Fe^{2+} ion irradiation at 500°C for nominal doses of ~20 and ~200 dpa. A parallel study using neutron irradiation at 300, 500, and 650°C for up to about 20 dpa is also in progress. The characterization and analyses of the low dose (~20 dpa) Fe^{2+} ion irradiated samples have been completed. The results indicate that the irradiation did not alter the crystalline nature of the nanoprecipitates. Particle dissolution, growth, and reprecipitation in different levels were observed after the irradiation. The radiation resistance of the carbide was much stronger than the nitrides in declined order TaC, VN, and TaN. TaC nanoprecipitates were observed to be much more resistant to irradiation than reported for a study using similar irradiation conditions. Post-irradiation examination of the high dose (~200 dpa) Fe^{2+} ion-irradiated and neutron-irradiated samples will be conducted and compared to the current observations.

PROGRESS AND STATUS

Introduction

MX-type precipitates have shown excellent coarsening resistance compared to Laves phase and chromium-rich $M_{23}C_6$ in 9-12% Cr ferritic-martensitic steels as well as RAF steels. They are critical for high temperature strength of this class of steels. Recently, however, limited data have shown the instability of MX, e.g., VN, TaC, and TaN, at elevated temperatures and irradiation conditions [1-4]. Three model alloys, favoring the formation of TaC, TaN, and VN nanoprecipitates, had been prepared to investigate the stability of these nanoprecipitates under thermal, stress, and irradiation conditions [5]. Thermal aging experiments at 600 and 700°C h for up to 5000 h had shown different levels of growth or dissolution for these nanoprecipitates [6]. The experimental progress assessing the radiation resistance of these nanoprecipitates is reported here.

Experimental Procedure

Mini-bars (2 x 2 x 20 mm^3) of the three model alloys Fe-1WVN, Fe-1WTaC, and Fe-1WTaN were machined using electro-discharge machining (EDM) with one of the longitudinal surfaces polished to mirror-finish for Fe^{2+} ion irradiation. The center region of the polished surfaces was irradiated using 5 MeV Fe^{2+} ions at 500°C for a nominal dose of ~20 dpa with a dose rate on the order of 10^{-4} s^{-1}, using the ion beam facility at University of Michigan through ATR National Science User Facility (ATR-NSUF).

The microstructures of the samples were characterized using transmission electron microscopy (TEM) in both conventional and scanning modes (STEM) on a FEI CM200 field-emission-gun TEM/STEM equipped with an EDAX energy dispersive X-ray spectroscopy (EDS) detector. TEM specimens, perpendicular to the polished surfaces, were lifted out and thinned to electron-transparent using focused ion beam (FIB) on a Hitachi NB5000. Specimen thickness of the characterized regions was estimated using convergent beam electron diffraction (CBED) technique.

Results

The ion irradiation damage to the alloy samples was simulated using the stopping and range of ions in matter software SRIM-2013 [7]. According to Stoller et al. [8], the "quick" Kinchin-Pease option, recommended displacement threshold energies, and zero lattice binding energy for each alloy element were used in the calculation. Figure 1 shows the calculated results with irradiation dose (dpa) as a function of depth into the TaC/TaN/VN samples. The depth distributions of the irradiation doped Fe concentration in atomic percentage (at.%) in respective alloys are also included. The Fe ion irradiation produces approximately the same displacement damage to the three alloy samples with damages gradually increasing from ~7.8 dpa at surface to a peak of ~48.8 dpa at a depth of 1.3 μm, and then quickly decreasing to 0 (unirradiated condition) at ~1.9 μm. The nominal dose of ~20 dpa is corresponding to the dose at half depth to the peak, which is schematically marked with a solid arrow. The irradiation doped Fe concentrations follow pseudo-Gaussian distributions with peaks, occurring behind the damage peak, at a depth of ~1.48 μm in the alloy samples. Slightly different amounts of doped Fe are shown in Fig. 1. It is expected that the amounts of doped Fe, <0.013 at.%, would not influence the microstructure and property of the alloy samples.

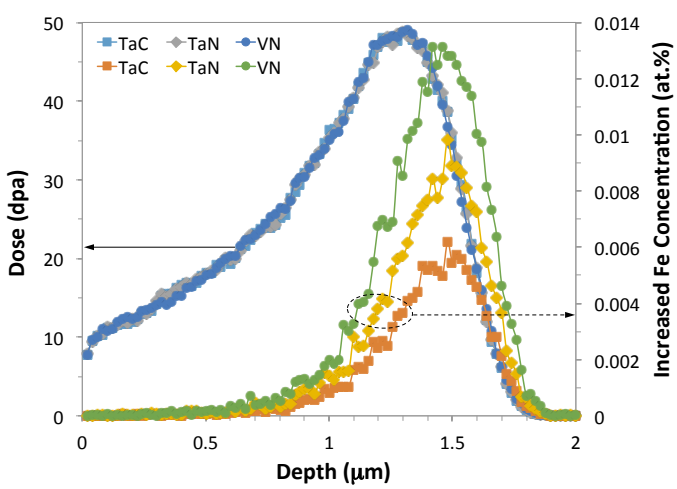

Figure 1. Simulated depth distribution of Fe ion irradiation damage dose (dpa) and doped Fe concentrations (at.%) in the model alloys TaC, TaN, and VN.

The microstructures of the model alloy samples prior to the Fe^{2+} ion irradiation are shown with the bright-field (BF) images in Figure 2. Many nanoprecipitates are uniformly distributed in the alloys. According to the selected area diffraction patterns (SADPs) and equilibrium phase calculation of the alloys, these nanoprecipitates are TaC, TaN, and VN in respective alloys.

Unlike the oval shape of the TaC nanoprecipitates, the TaN and VN nanoprecipitates were found to be in disk shape despite their spherical appearance resulted from their adjacent strain field. The longest side of the nanoprecipitates was used in the statistical particle size measurement. The CBED estimated specimen thickness was assumed to be uniform within the characterized regions. The volumetric number density and size of the nanoprecipitates were analyzed and plotted in Figure 4.

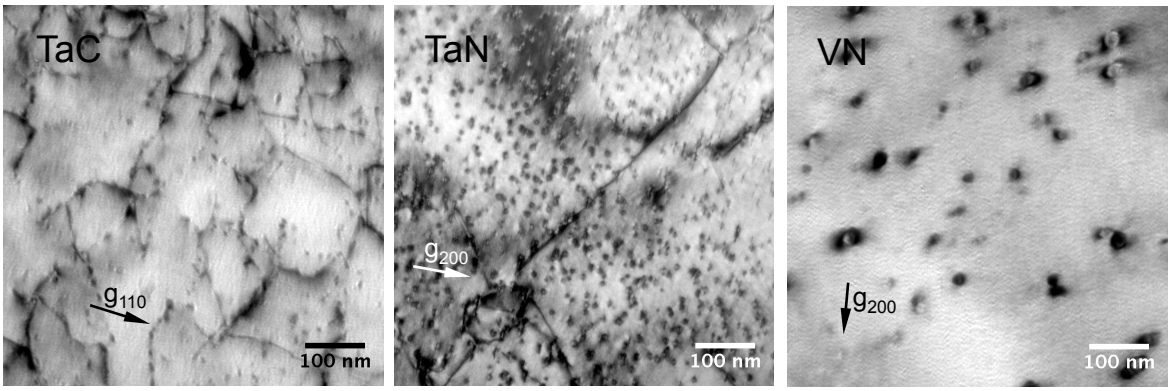

Figure 2. BF images of the unirradiated model alloys showing the distribution of the TaC, TaN, and VN nanoprecipitates.

High-angle annular dark field (HAADF) STEM was used to characterize the TaC nanoprecipitates. The Z-contrast imaging technique was found to be suitable for TaC, which captured the TaC distribution throughout the irradiated depth. Figure 3a shows a HAADF-STEM image of TaC irradiated to ~20 dpa at half-depth to the damage peak. The black arrow denotes the irradiation direction. The HAADF-STEM contrast of TaN was not as good as TaC, which was even worse for VN because of the lower weight (or Z) of V compared to Ta. Therefore, dark-field (DF) imaging using the beam condition as shown in Fig. 3 was employed to characterize TaN and VN. Figures 3b and 3c exhibit the DF images of TaN and VN, respectively, irradiated for ~20 dpa at half-depth to the damage peak. The white particles of TaN and VN are approximately parallel to the irradiation direction. This orientation relationship was not a result of the irradiation because other orientation relationship, e.g., approximately perpendicular to the irradiation direction, was also observed in other grains.

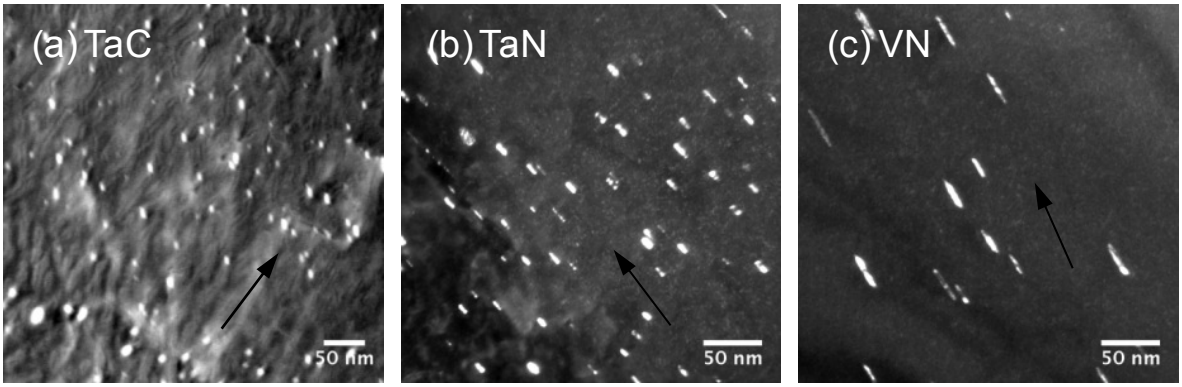

Figure 3. (a) HAADF (STEM) and (b-c) DF (TEM) images of the TaC, TaN, and VN irradiated to ~20 dpa. The arrow on each image indicates the irradiation direction.

The density and average size of the TaC, TaN, and VN nanoprecipitates after ~20 dpa irradiation are plotted in Figure 4 in solid symbols, comparing to the data in the unirradiated condition in open symbols. Slight dissolution (smaller size) with some reprecipitation (larger density) were observed for the TaC nanoprecipitates after the irradiation. In contrast, the irradiation resulted in some increase in density with significant growth in size of VN. The large standard deviation of size may also suggest the coexistence of particle growth and reprecipitation. However, TaN had slightly decreased size, together with significantly decreased density, suggesting primary dissolution of TaN after the irradiation.

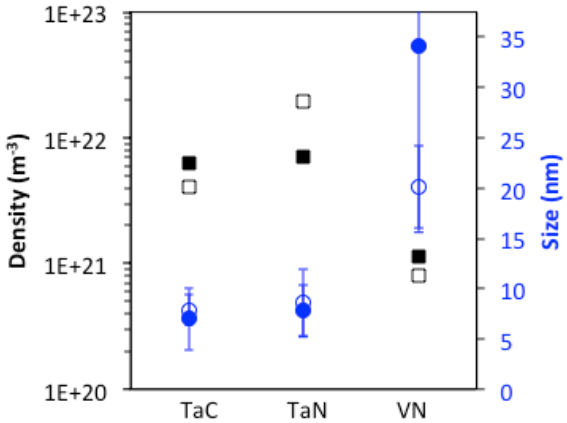

Figure 4. Particle density (black squares) and size (blue circles) after ~20 dpa irradiation (solid symbols) compared to the initial unirradiated condition (open symbols) of TaC, TaN, and VN nanoprecipitates.

The relatively good radiation resistance of TaC nanoprecipitates was inconsistent with the literature reported predominant dissolution of TaC after Fe^{3+} ion irradiation of Fe-0.2Ta-0.015C alloy at 500° for ~20 dpa [3,4] and neutron irradiation of ORNL9Cr-2WVTa and JLF-1 RAF steels at 300°C for ~5 dpa [3,4]. The predominant dissolution of TaC in the neutron-irradiated RAF steels may attributable to the lower irradiation temperature, lower particle volume fraction, and more likely to be the nature of Ta(C,N) rather than TaC, due to the presence of relatively

high nitrogen content in the steels, as suggested in this study that the radiation resistance of nitride is inferior to carbide. The slightly lower particle volume fraction in Fe-0.2Ta-0.015C alloy may have favored the greater dissolution of TaC compared to the observations in this work. However, the lower volume fraction should not result in the dominant dissolution of TaC. Other factors, e.g., irradiation temperature, displacement rate, etc., may have also played roles.

Fe^{2+} ion irradiation of the alloy samples for a nominal dose of ~200 dpa has been completed recently. The microstructural characterization and analysis will be conducted in the same way to have a clear picture regarding the radiation resistance of these MX-type nanoprecipitates. Neutron irradiation of the alloy samples will be finished soon. The effect of dose, dose rate, and irradiation temperature on particle stability will be explored.

REFERENCES

[1] M. Tamura, H. Sakasegawa, A. Kohyama, H. Esaka, and K. Shinozuka, *J. Nucl. Mater.* **329**, 328 (2004).
[2] A. Kabadwal, M. Tamura, K. Shinozuka, and H. Esaka, *Metall. Mater. Trans. A* **41**, 364 (2010).
[3] H. Tanigawa, H. Sakasegawa, and R. L. Klueh, "Irradiation Effects on Precipitation in Reduced-Activation Ferritic/Martensitic Steels," *Mater. Trans.* **46**, 469-474 (2005).
[4] H. Tanigawa, H. Sakasegawa, H. Ogiwara, H. Kishimoto, and A. Kohyama, "Radiation Induced Phase Instability of Precipitates in Reduced-Activation Ferritic/Martensitic Steels," *J. Nucl. Mater.* **367-370**, 132-136 (2007).
[5] L. Tan, "Stability of Strengthening Precipitates in Model Ferritic Steels," Semiannual Progress Report, DOE/ER-0313/52, June 30, 2012.
[6] L. Tan, Y. Katoh, and L. L. Snead, "Stability of Nanoprecipitates in Fe-Base Model Alloys," Semiannual Progress Report, DOE/ER-0313/53, December 31, 2012.
[7] The Stopping and Range of Ions in Matter (SRIM) (http://www.srim.org).
[8] R. E. Stoller, M. B. Toloczko, G. S. Was, A. G. Certain, S. Dwaraknath, and F. A. Garner, "On the Use of SRIM for Computing Radiation Damage Exposure," *Nucl. Instrum. Methods Phys. Res. B* **310**, 75-80 (2013).